

# High-resolution, high-speed, low data age uncertainty, heterodyne displacement measuring interferometer electronics

Frank C Demarest

Zygo Corporation, Laurel Brook Road, Middlefield, CT 06455, USA

Received 30 September 1997, in final form 10 March 1998, accepted for publication 3 April 1998

**Abstract.** An advanced displacement measuring interferometer system has been developed to satisfy the needs of semiconductor manufacturing and lithography. The system electronics provides a position resolution of 0.31 nm at velocities up to  $2.1 \text{ m s}^{-1}$  when the system is used with a double-pass interferometer. Output data rates up to  $10^7$  samples per second are available. The data age, which is the delay from the interferometer optics to the measurement sample, can be adjusted to equalize differences between axes to within 1 ns. This low data age uncertainty is necessary for high-resolution, high-speed, multiple-axis measurements.

**Keywords:** phase meters, heterodyne interferometry, laser measurement systems, photolithography

## 1. Introduction

The use of interferometry to measure changes in position, length, distance and optical length is well known [1, 2]. A typical displacement measuring interferometer system consists of a frequency-stabilized laser light source, interferometer optics and measuring electronics. The interferometer optics splits the laser light into a reference path and a measurement path, then recombines the light returning from the two paths and directs it to a photodiode where it produces an interference signal. A distance change of one wavelength in the measurement path relative to the reference path produces a phase change of  $360^\circ$  in the interference signal. The measuring electronics measures and accumulates the phase and provides a position output for the application.

For many leading edge applications, such as, in the step-and-scan photolithography tools used to manufacture integrated circuits, many axes of motion must be measured interferometrically at high velocity and with high resolution. The number of measurement axes requiring interferometric metrology is growing from two to three per system a few years ago to eight axes today and to 15–20 axes in the future. An advanced photolithography system may include measurement of  $X$ ,  $Y$ , pitch and yaw for each of two stages. The angular measurements are required for compensation of Abbé errors.

The accuracy requirements increase as the size of integrated circuit features decreases and the die size

and wafer size increase. The need for a high measurement velocity is a result of the increasing throughput requirements of these systems. Multiple-axis measurements at high velocity require that position measurements be simultaneous within a very short time interval (low data age uncertainty). This paper describes the measurement electronics for an interferometer system that satisfies these needs for high-resolution, high-speed, low data age uncertainty measurements.

### 1.1. A description of the system

The heterodyne interferometer system is shown in figure 1. The laser head generates a pair of collinear, orthogonally polarized, optical beams of equal intensity differing in frequency by  $F_R$ , which is the 20 MHz reference frequency in this system. The optical beams pass through an interferometer configured to measure the length or position of interest. For simplicity, figure 1 shows a simple linear displacement interferometer; other configurations may also be used [3]. The polarization beamsplitter (PBS) reflects one polarization of the incoming light to a stationary retroreflector ( $RR_1$ ), and passes the other polarization of light to a movable retroreflector ( $RR_2$ ). The retroreflectors return the light to the polarization beamsplitter (PBS), where one beam is transmitted and the other beam is reflected, so that the two beams are again collinear. Linear motion of the movable retroreflector ( $RR_2$ ) results in a

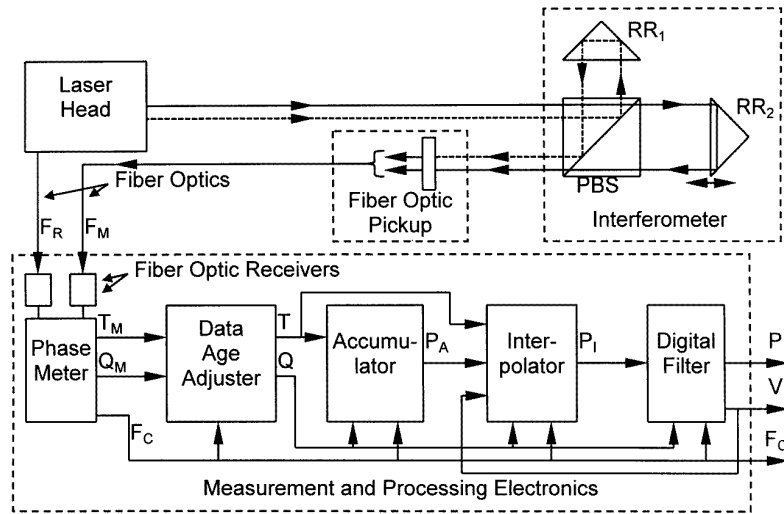


**Figure 1.** A block diagram of the system showing the laser source, interferometer and measurement electronics.

corresponding change in the difference in phase between the two beams.

The output beams from the interferometer go to a fibre-optical pick-up. There they pass through a polarizer that mixes the parallel and overlapping portions of the beams and a lens that couples the light into an optical fibre. The processing electronics contains a fibre optical receiver that produces an electrical measurement signal corresponding to the optical signal. The measurement signal has a frequency which is equal to the reference frequency  $F_R$  plus the Doppler shift frequency, or

$$F_M = F_R \pm nv/\lambda \quad (1)$$

where  $v$  is the velocity of the interferometer element whose position is being measured,  $\lambda$  is the wavelength of light and  $n$  equals 2, 4, etc depending on the number of passes the light makes through the interferometer. In the example of figure 1, the movement of the retroreflector  $RR_2$  produces the Doppler shift and  $n$  is equal to 2.

The laser head also outputs the reference signal  $F_R$  via a fibre-optical cable that goes to a fibre-optical receiver in the processing electronics. The use of fibre optics for the signals to the processing electronics eliminates problems due to electro-static discharge (ESD) and sources of electrical noise in the application environment. The electronics measures the phase difference and processes it to provide position and velocity outputs. The processing consists of four sections.

(i) The data age adjuster advances or retards the apparent time that the measurement occurs so that multiple channels may be adjusted to have identical time delays, compensating for differences in optical path, length of optical fibre and electronics.

(ii) The accumulator converts two consecutive phase measurements into a change of ( $\Delta P$ ) position measurement representing the distance travelled between the two measurement times, then sums the  $\Delta P$  measurements to provide an accumulated position value.

(iii) The interpolator adjusts the position measurements to compensate for the time difference between when the measurement occurred and when the system's clock processed the measurement.

(iv) The digital filter reduces the noise in the measurement and provides a constant data rate for the output position and velocity values.

All of the measurement and processing electronics is packaged on a single 6U (160 mm  $\times$  233 mm) VMEbus circuit board assembly. The processed digital position and velocity values are available either on the VMEbus or on a proprietary 32-bit parallel bus.

## 1.2. Requirements on the system

Current and future applications for distance measuring interferometers require much better performance than that of previously available systems. Satisfying these more demanding requirements requires a new technical approach to the measurement. The following specification goals were chosen after a review of current and future potential applications [4] and technological limitations.

(i) A maximum operating velocity of  $\pm 2.2$  m  $s^{-1}$  when using a double-pass interferometer. This corresponds to a Doppler shift of  $\pm 13.9$  MHz. The dynamic accuracy over this velocity range should be equal to the static accuracy. This velocity range is four times greater than that of any other commercially available system.

(ii) A position resolution of 0.31 nm ( $\lambda/2048$ ) when using a double-pass interferometer. This corresponds to a phase resolution of  $360^\circ/512$ , or  $0.7^\circ$ , which is 97.7 ps at 20 MHz. This position resolution is a factor of two better than that of any other commercially available system.

(iii) Data age differences among axes less than  $\pm 2$  ns for accurate dynamic measurements using multiple axes. This data age uncertainty is a factor of five better than that of any other commercially available system.

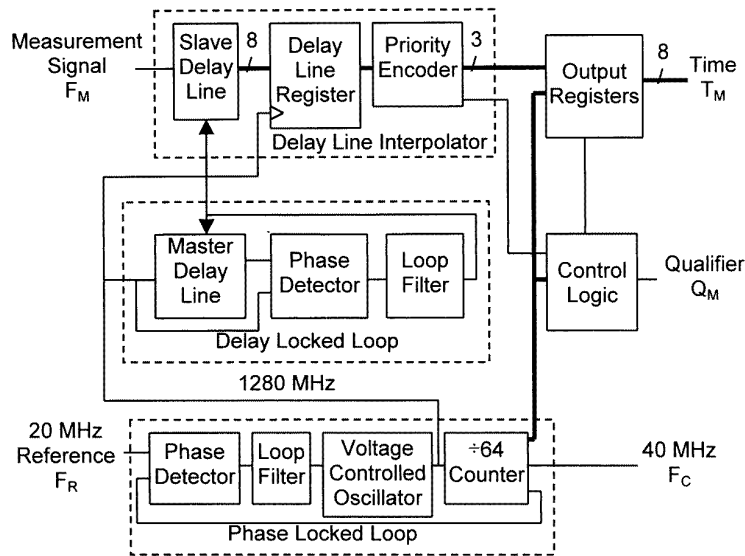


Figure 2. The block diagram of the phase meter.

These performance goals were technically challenging to implement. The wide operating frequency range means greater noise in the measurement, making the fine position resolution more difficult to achieve. The high operating frequency requires faster processing electronics and the high resolution requires word sizes of 36 bits or more in the digital processing, making the implementation of the digital filter more difficult.

## 2. High-velocity measurement

The maximum measurement velocity is usually limited by the difference in frequency between the two components of the laser beam. Interferometers using a Zeeman-split laser source are typically limited to a Zeeman difference frequency of 3–4 MHz, which corresponds to approximately  $\pm 0.5 \text{ m s}^{-1}$  with a double-pass interferometer. An interferometer using an acousto-optical modulator (AOM) in the laser source [5] has a frequency difference defined by the AOM driving frequency. The AOM driving frequency chosen is 20 MHz. The signal processing electronics was designed for a frequency range of  $20 \pm 13.3 \text{ MHz}$ , corresponding to a maximum velocity of  $\pm 2.1 \text{ m s}^{-1}$  with a double-pass interferometer.

There are many ways to measure the phase of the signal in a displacement measuring interferometer [6, 7]. Analogue phase measurement is difficult to implement with good dynamic accuracy over the wide frequency range required (6.7–33.3 MHz, a 5:1 range) and may also suffer from drift, nonlinearity, noise and cross talk in the electronics. Digital phase measurement, described in the next section, maintains the required accuracy and resolution over the full measurement velocity range.

## 3. High-resolution measurement

The system's resolution is limited by the system's noise and by the phase measurement method. The requirement

for high-velocity measurements and the corresponding wide measurement frequency range make high-resolution measurements more difficult.

The receiver shown in figure 1 converts the optical signal from the interferometer into an electrical signal. The bandwidth of the receiver is put equal to the measurement frequency range in order to reduce the noise in the measurement signal.

The phase measurement is performed by a custom-built emitter-coupled logic (ECL) application-specific integrated circuit (ASIC) phase meter. The phase meter measures the time of occurrence of the rising edge of the measurement signal relative to the 40 MHz system clock.

The block diagram of the phase meter is shown in figure 2. The phase-locked loop (PLL) generates a 1280 MHz internal clock derived from the 20 MHz reference from the laser head. The delay line interpolator measures the time of occurrence of the rising edge of the measurement signal relative to the 1280 MHz clock with a resolution of an eighth of the clock period, or 97.7 ps. It does this by passing the measurement signal through a tapped delay line and sampling the contents of the delay line once per clock cycle. After a measurement edge has occurred, the delay line register contains an 8-bit pattern representing where the signal was in the delay line at the time of the next clock cycle. The priority encoder converts this pattern into a 3-bit binary value. The 3-bit output is combined with the lower 5 bits of the divide-by-64 counter in the PLL. The resulting 8-bit output from the phase meter represents the time of occurrence of the measurement signal within the 40 MHz system clock period.

The delay-locked loop (DLL) adjusts the control voltage for the master delay line so that the delay is equal to one period of the 1280 MHz clock. The same control voltage adjusts the delay of the slave delay line used in the delay line interpolator so that the interpolator works properly even with variations in chip processing, chip temperature or power supply voltage.

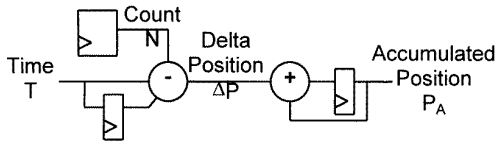


**Figure 3.** The position accumulator converts the time value from the phase meter into a position value.

The outputs of the phase meter are an 8-bit digital time value representing a fraction of the 40 MHz clock period, a qualifier bit which indicates that a measurement edge occurred during that clock cycle and the 40 MHz system clock. The phase meter outputs go to the interface ASIC, which is a custom-built CMOS gate array containing all of the digital signal processing and the bus interfaces.

The position accumulator shown in figure 3 converts two consecutive time values ( $T_1$  and  $T_2$ ) from the phase meter and the count of 40 MHz system clock cycles elapsed between them ( $N$ ) into a change in phase value ( $\Delta\phi$ ). The 8-bit time resolution corresponds to 9-bit, or 1 part in 512, phase resolution of the 20 MHz reference signal period. This phase resolution determines the position resolution of  $\lambda/(512n)$ , where  $\lambda$  is the wavelength of light, and  $n$  equals 2, 4, etc depending on the number of passes the light makes through the interferometer. The ( $\Delta\phi$ ) values are numerically identical to ( $\Delta P$ ) values:

$$\Delta P = \Delta\phi = 256(1 - N) + T_1 - T_2. \quad (2)$$

The  $\Delta P$  values are accumulated to produce an accumulated position value ( $P_A$ ):

$$P_A = \sum(\Delta P). \quad (3)$$

The phase measurement has a dynamic error due to the variation between the time when the measurement signal transition occurred and when it is processed synchronously with the system clock. This time variation of  $\pm 1/2$  of the system clock's cycle results in a random position error, which appears as system noise proportional to the velocity. The position interpolator shown in figure 4 calculates and subtracts this dynamic error:

$$P_I = P_A - TV. \quad (4)$$

The time value  $T$  is derived from the output of the phase meter and the velocity value  $V$  is provided by the digital filter. This calculation has a precision eight times finer than the system's resolution so that it is not a limitation on performance.

The interpolated position value  $P_I$  passes through the digital filter shown in figure 5. This filter design has the useful property that, for a constant velocity, there is no time delay between the input and the output. This filter architecture is similar to that described by Benedict and Bordner [8] and is also known as the alpha-beta filter [9]. The choice of a  $K_p$  (position, or proportional) gain value from  $2^{-2}$  to  $2^{-9}$  selects a filter bandwidth from 3.8 MHz to 15 kHz and a corresponding  $K_v$  (velocity, or integral)

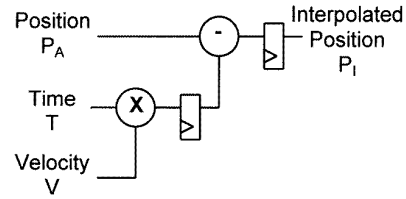


**Figure 4.** The position interpolator corrects for the dynamic error due to variation in the time difference between the measurement signal and the system's clock.

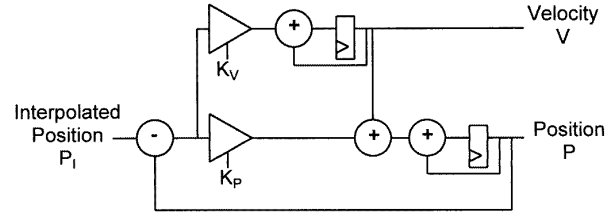


**Figure 5.** The digital filter provides position and velocity outputs.

gain value from  $2^{-6}$  to  $2^{-20}$  is chosen for the best stability and dynamic response. For typical operation, a  $K_p$  value of  $2^{-6}$  and a  $K_v$  value of  $2^{-14}$  provide a bandwidth of 128 kHz. The filtered output can be read by access to the board through the VMEbus or through a proprietary 32-bit bus interface at rates up to  $10^7$  32-bit transfers per second.

#### 4. Compensation for data age

Some applications such as angle measurements require two or more measurement axes in order to provide the necessary information. To achieve full accuracy with dynamic multi-axis measurements, all measurements must have the same 'data age', which means that they represent the same instant in time. For example, at a velocity of  $2 \text{ m s}^{-1}$ , a difference in data age of 1 ns between two measurement signal paths produces a position error of 2 nm, six times greater than the system's resolution.

Multiple-axis measurements are synchronized by a common reference provided to all phase meters and by a common sample control signal. The variation in data age among axes is then due to differences in the measurement electronics, the measurement electrical and optical signal paths and the reference signal path.

Differences in data age among axes must be minimized or eliminated. An all-digital method for adjusting the data age of each axis fulfils this requirement (USA and foreign patents are pending). This adjustment has a time resolution equal to the phase meter's resolution of 97.7 ps.

The block diagram of the data age adjuster is shown in figure 6. The output from the phase meter represents the time of occurrence of a zero crossing of the measurement signal relative to the 40 MHz system clock. The left-hand portion of figure 6 adjusts the data age by fine amounts of a fraction of a clock period. Adding a constant to the time value is equivalent to adding a corresponding time delay to

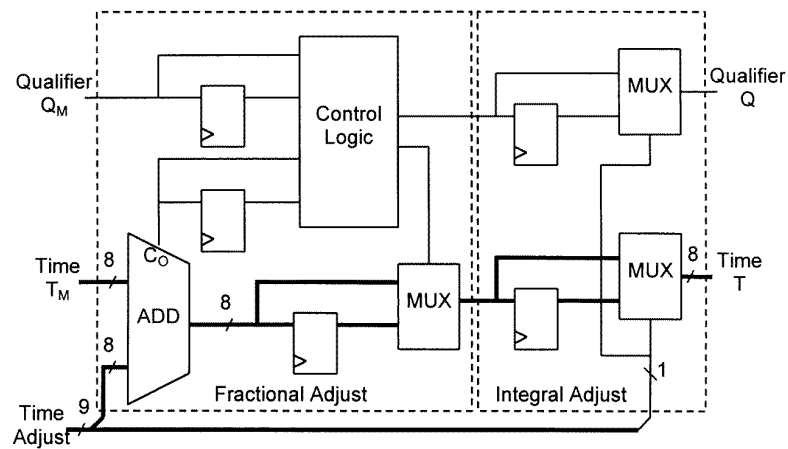


**Figure 6.** The data age adjuster digitally compensates for propagation delays in the optics and electronics.

the measurement path. If the addition results in a carrying over, the control logic causes the data to be output one clock period later. The right-hand half of figure 6 adjusts the data age by amounts equal to one clock period by selecting output of the data one clock period later. Additional stages can be cascaded if greater adjustment of the data age is required.

The measurement board test and calibration procedure includes measuring the delay of the measurement and reference signals and storing the values in an on-board electrically erasable programmable read-only memory (EEPROM). During initialization of the system, the data age adjustment values for each axis are calculated and loaded into the hardware. The adjustment can also include known differences in optical or fibre-optical path lengths.

Distortion of the group delay in the bandpass filter in the fibre-optical receiver can also affect the data age of the measurement. The group delay is the time required for a signal at a given frequency to pass through a circuit. Mathematically stated, the group delay is the derivative of the phase with respect to frequency. A filter with a linear phase versus frequency characteristic will have a constant group delay. If the group delay is not constant, the measurements taken along axes operating at different velocities will represent different instants in time. The bandpass filter and related electronics were designed to have a group delay constant to within  $\pm 1$  ns over the entire measurement frequency range.

## 5. Performance

The high performance of this system, combined with new considerations such as the dynamic accuracy and data age, required development of a new test system and new test methods. Simulated signals from signal generators are used for most tests since they provide good accuracy and programmability and eliminate other sources of system error. Two different types of signal generators were needed to satisfy all the test requirements. The desired generator output signals are converted to amplitude-modulated optical

**Table 1.** The typical performance.

Test	Typical performance		
Maximum error	$\pm 1.2LSB$	$\pm 0.84^\circ$	$\pm 0.37$ nm
Mean standard deviation	$0.23LSB$	$0.16^\circ$	$0.07$ nm
Grand standard deviation	$0.36LSB$	$0.25^\circ$	$0.11$ nm
Percentage no noise	50%		
Number of quiet intervals	512		
Dynamic accuracy	$0.36LSB$	$0.25^\circ$	$0.11$ nm
Sensitivity	$2.8 \mu W$		
Data age compensation	$\pm 0.3$ ns		

signals that simulate the laser reference signal and the measurement signal.

Static tests use two synthesized signal generators (Hewlett-Packard 3325B), one for the reference signal and one for the measurement signal. These generators are synchronized by a common external reference source and provide adjustable output phase in  $0.1^\circ$  steps, but are limited to a maximum output frequency of 21 MHz.

Dynamic tests use an arbitrary function generator (Tektronix AFG-2020). This generator has two independent synchronized outputs and has a maximum output frequency of 100 MHz with programmable frequency sweeps, but does not have an adjustable output phase.

For most tests, the digital filter bandwidth is set to 128 kHz and optimum signal levels are used. All test results reported in nanometres assume the use of a double-pass interferometer. The system resolution least significant bit (LSB) is equal to  $0.7^\circ$  or 0.31 nm. The typical performance is summarized in table 1.

### 5.1. The static accuracy

The static accuracy test applies a measurement signal while the phase is stepped from zero to  $360^\circ$  in  $0.1^\circ$  steps. At each phase step, 100 position readings are recorded. The position error is calculated by converting the phase angle into an equivalent position value and subtracting it from the measured position. For each group of 100 readings, the mean and standard deviation are calculated. Figure 7

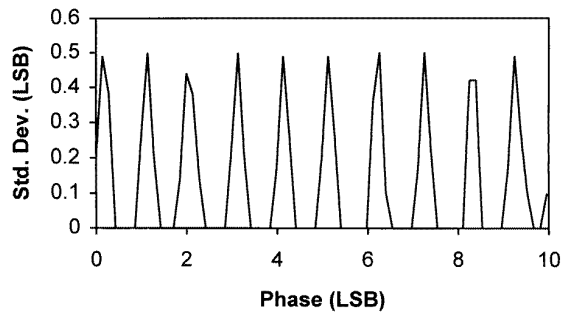


**Figure 7.** The standard deviation versus the phase, illustrating the periodic variation due to quantization.

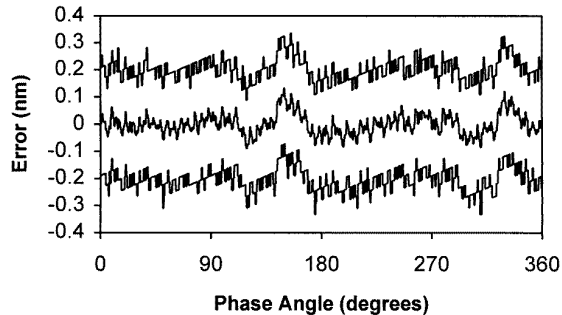


**Figure 8.** The typical accuracy, showing the maximum error, average error and minimum error versus the phase angle.

shows that, as the phase is stepped, the standard deviation has a periodic variation between zero, representing a stable value, and 0.5, representing dithering between two adjacent values. The resulting data are processed to provide the following performance indicators.

(i) The maximum error is the worst-case difference between the calculated ideal position output value and the actual position output value. This includes quantization errors ( $\pm 0.15$  nm) and signal generator errors ( $\pm 0.087$  nm). Figure 8 shows the maximum error and the average error for a typical system. Typical results are  $\pm 0.37$  nm.

(ii) The mean standard deviation is the RMS mean of all of the standard deviation values. The result of this calculation is an indicator of the sharpness of the quantization performed by the phase meter and is insensitive to periodic errors. In an ideal and noiseless system this value would be nearly zero; typical results are 0.071 nm RMS.

(iii) The grand standard deviation is the standard deviation of the position error at all phase steps. This is an indicator of quantization errors plus periodic errors. In an ideal system, this would be 0.090 nm RMS; typical results are 0.11 nm RMS.

(iv) The percentage no noise is the percentage of phase steps for which the standard deviation is zero. This result is inversely related to the mean standard deviation. In an ideal system, this would be nearly 100%; typical results are 50%.

(v) The number of quiet intervals is the number of intervals for which the standard deviation is zero. In an

A high-resolution displacement measuring interferometer

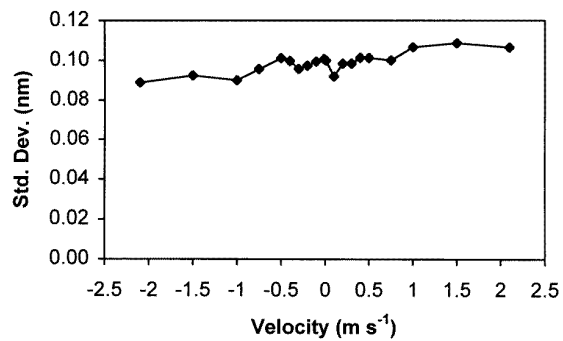


**Figure 9.** The dynamic accuracy is nearly constant over the entire range of the measurement velocity.

ideal system this would be 512, but typically it may be as high as 520 due to measurement and test system noise.

## 5.2. The dynamic accuracy

The dynamic accuracy test uses the arbitrary function generator to simulate a stage moving at a constant velocity. One channel provides a fixed 20 MHz reference and the other channel is programmed to ramp up or down to the specified frequency. At each frequency, 500 position and time data points are recorded and a least squares fit to a line is performed. The standard deviation of the position error between the line and the 500 points is recorded for each simulated stage velocity. The plot of the dynamic accuracy versus the velocity is shown in figure 9. Typical results are 0.099 nm RMS near zero velocity and 0.11 nm RMS at the maximum velocity.

## 5.3. The sensitivity

The static accuracy tests are performed with optimum signal levels. For an actual multiple-axis application, the laser output of typically 500  $\mu$ W must be split to provide light for each axis. Light is also lost in the optics and fibre-optical receiver and due to misalignment of the interferometer. The system sensitivity measurement provides an indication of the amount of light necessary to produce reliable measurements.

This test measures the static accuracy over a range of simulated signal levels. As the signal level is reduced, the standard deviation of the measurement increases. Interpolation is used to determine the signal level that will result in a grand standard deviation (described earlier) of 0.28 nm RMS. This signal level is sufficient to give reliable measurements, but has greater noise than that with normal signal levels.

To determine the relationship between the simulated signal level and the equivalent optical power, a laser source with a variable optical attenuator is used. During the sensitivity test, the readings from the signal strength measurement output of the fibre-optical receiver are recorded for each signal level. Then the laser source is used with the variable attenuator adjusted to produce readings with the same signal strength and the optical power into the fibre-optical pick-up is measured and recorded.

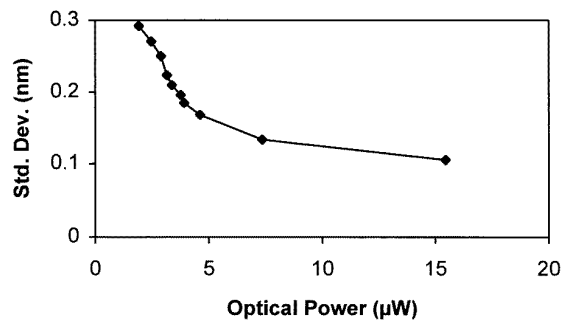


**Figure 10.** The measurement noise versus the optical power.

The typical sensitivity is  $2.8 \mu\text{W}$ ; a typical graph of the standard deviation versus the optical power is shown in figure 10.

#### 5.4. Compensation for the data age

The data age compensation test measures the uncertainty in data age between axes. The arbitrary function generator provides a simulated measurement signal that starts at 20 MHz (zero velocity), ramps to 27 MHz and then ramps to 13 MHz. The signal is coupled to two measurement axes by a fibre-optical splitter with two outputs of equal length. The reference and measurement delay values that were measured during the board test and calibration are used to calculate the data age adjustment settings. At each velocity, both measurement axis positions are simultaneously sampled. The data age error is calculated as

$$t = \Delta P / V. \quad (5)$$

The calculated data age error was within a range of  $\pm 0.3$  ns, which is the resolution of the calculations.

Another test involved addition of a fibre-optical cable of known length to one measurement axis and the data age error was measured. This value was equal to that calculated from the fibre-optical length and the refractive index. After the data age registers had been set to eliminate this error, the measured data age error was less than  $\pm 0.3$  ns.

#### 5.5. System noise

The system noise test measures phase stability over a 15 min period in a normal laboratory environment. The signal source is a standard laser head. The reference signal from the laser head is connected to the reference

input of the measurement board through a 3 m fibre-optical cable. The laser signal from the laser head goes directly to a fibre-optical pick-up and is connected to the measurement input of the measurement board through a second 3 m fibre-optical cable. In this configuration there is no interferometer, so any noise or drift can be attributed to the laser head or measurement electronics. The measured variation in position during this test was 0.31 nm (maximum minus minimum).

## 6. Conclusion

The electronics for a heterodyne displacement measuring interferometer system for the high-resolution, high-speed, low data age uncertainty requirements of semiconductor manufacturing and other demanding applications has been described. The measured performance confirms that this system will satisfy the needs of present and applications and of those expected to arise in the future.

## Acknowledgments

The contributions and encouragement by Kurt Redlitz and the DLL design by Germán Gutierrez are gratefully acknowledged.

## References

- [1] Sommargren G E 1987 A new laser measurement system for precision metrology *Precision Eng.* **9** 179–84
- [2] Bobroff N 1993 Recent advances in displacement measuring interferometry *Meas. Sci. Technol.* **4** 907–26
- [3] Zaroni C 1989 Differential interferometer arrangements for distance and angle measurements: principles, advantages and applications *VDI-Ber.* **749** 93–106
- [4] Semiconductor Industry Association 1997 *The National Technology Roadmap for Semiconductors* (San Jose, CA: The Semiconductor Industry Association) pp 82–98
- [5] Sommargren G E 1987 Apparatus to transform a single frequency, linearly polarized laser beam into a beam with two, orthogonally polarized frequencies, USA Patent 4684828
- [6] Oldham N M, Kramar J A, Ketrick P S and Teague E C 1993 Electronic limitations in phase meters for heterodyne interferometry *Precision Eng.* **15** 173–9
- [7] Oka K, Tsukada M and Ohtsuka Y 1991 Real-time phase demodulator for optical heterodyne detection processes *Meas. Sci. Technol.* **2** 106–10
- [8] Benedict T R and Bordner G W 1962 Synthesis of an optimal set of radar track-while-scan smoothing equations *IRE Trans. Automatic Control* July 27–32
- [9] Penoyer R 1993 The alpha–beta filter *C User's J.* July 73–86